Article

Soil from an Abandoned Manganese Mining Area (Hunan, China): Significance of Health Risk from Potentially Toxic Element Pollution and Its Spatial Context

Xin Luo [1,2], Bozhi Ren [1,2,*], Andrew S. Hursthouse [1,3], Jonathan R. M. Thacker [4] and Zhenghua Wang [1,2]

1   Hunan Provincial Key Laboratory of Shale Gas Resource Exploitation, Xiangtan 411201, China; luoxin@mail.hnust.edu.cn (X.L.); andrew.hursthouse@uws.ac.uk (A.S.H.); wzh@hnust.edu.cn (Z.W.)
2   School of Civil Engineering, Hunan University of Science and Technology, Xiangtan 411201, China
3   School of Computing Engineering & Physical Sciences, University of the West of Scotland, Paisley PA1 2BE, UK
4   School of Health & Life Sciences, University of the West of Scotland, Paisley PA1 2BE, UK; richard.thacker@uws.ac.uk
*   Correspondence: bozhiren@126.com; Tel.: +86-137-8742-7077; Fax: +86-0731-5829-0182

check for updates

Abstract: This study assessed the significance and potential impact of potentially toxic element (PTE) (i.e., Mn, Pb, Cu, Zn, Cr, Cd, and Ni) pollution in the surface soil from an abandoned manganese mining area in Xiangtan City, Hunan Province, China, on the health of residents. The risks were sequentially evaluated using a series of protocols including: the geo-accumulation index (I_{geo}), pollution load index (PLI), potential ecological risk index (RI), and implications for human health from external exposures using the hazard quotient (HQ), hazard index (HI) and carcinogenic risk (CR). The results revealed that Mn and Cd were the major pollutants in the soil samples. The ecological risk assessment identified moderate risks, which were mainly derived from Cd (82.91%). The results of the health risk assessment revealed that generally across the area, the non-carcinogenic risk was insignificant, and the carcinogenic risk was at an acceptable level. However, due to local spatial fluctuation, some of the sites presented a non-carcinogenic risk to children. The soil ingestion pathway is the main route of exposure through both non-carcinogenic and carcinogenic risks, with Mn being the major contributor to non-carcinogenic risk, with Cr and Cd the major contributors to carcinogenic risk. In addition, three pollution sources were identified through the Pearson correlation coefficient and principal component analysis (PCA), which included: a. mining activities and emissions from related transportation; b. natural background; c. agricultural management practices and municipal sewage discharge. The study provides information on the effects of spatial variation for the development of the abandoned mining areas and a useful approach to the prioritization of locations for the development and utilization of soil in these areas in China.

Keywords: abandoned manganese mine; potentially toxic element; spatial distribution; ecological risk assessment; source analysis; health risk assessment

1. Introduction

The impact of pollution from a range of potentially toxic elements (PTEs) on humans and wider ecosystems remains a major concern for society [1]. Many PTEs are found in the soil and rocks in nature, but most significant are the releases into soil from various human activities [1], such as mining activities (mining and smelting), agricultural production (application of pesticides, herbicides),

industrial activities, transport emissions, etc. [1–3]. Enriched levels can have a number of impacts such as creating wasteland, and affecting the growth and reproduction of biological organisms [1]. In addition, PTEs in the soil can enter the human body through the enrichment in the food chain, direct ingestion, dermal contact and inhalation, and eventually cause harm to the human body and cause various diseases [1,4,5]. Some relevant examples are the accumulation of Mn in the human body which can cause mental illness and even Parkinson's syndrome [6]; excessive Cd can cause renal insufficiency and prostate disease [2] and the accumulation of Pb can lead to high circulation in the blood and damage the endocrine and immune systems [1,7]. Excess Cu can affect liver and kidney function and even be fatal [1,6]. Thus, where enrichment exists, it is important to evaluate the significance of the pollution and undertake a more detailed risk assessment [8,9].

The manganese mining area in Xiangtan City has been producing manganese ore since 1913, providing a significant manganese resource for the country [10], but recently, production has stopped. To re-use previously impacted land it is necessary to evaluate the pollution levels and risk to the environment in order to achieve faster and better development. There are already many studies on the risk assessment of soil from mining, urban use, and for food production [1,8,9]. However, studies on the impact of risk assessment on future land use and its spatial variation are not common. In addition, the use of the geo-accumulation index (I_{geo}) can not only reflect the natural changes in the distribution of single PTEs, but also demonstrate the impact of human activities on pollution by PTEs. The pollution load index (PLI) directly apportions the contribution of a single PTE to the combined pollution across the study area. The potential ecological risk index (RI) is one of the most commonly used methods to evaluate ecological risk. This method takes into account the combined effects of the concentration of potentially toxic elements and toxic response factors.

Since there is no clear health risk assessment method in China, the method recommended by EPA for health risk assessment was adopted, which includes the hazard quotient (HQ), and hazard index (HI), and carcinogenic risk (CR). The use of multivariate analysis such as principal component analysis (PCA) allows relationships between variables to be highlighted and when combined with the Pearson correlation coefficient, presents a good method of source apportionment. Therefore, this study reports on the assessment of risk from the potential reuse of soil in an abandoned mining area, through the use of a series of environmental and human health risk assessment methods including geo-accumulation index (I_{geo}), pollution load index (PLI), potential ecological risk index (RI), HQ, HI, CR. The Kriging interpolation method was used to derive the spatial distribution of PTEs in the soil in the study area using ArcGIS 10.3. This study extends our foundation work in the region supporting the re-development and utilization of soil in the abandoned manganese mining area in Xiangtan. The spatial assessment provides direction for soil development and utilization and serves as a template for risk assessment in other mining areas in China [5,10,11].

The main objectives of this study were to: (1) assess the potential ecological risks of the local environment and the health risks to local residents from external exposure in a sub region of the mining area; (2) evaluate the significance of the PTE levels in the soil in the study area; (3) demonstrate spatial variability and its significance; (4) identify the source of seven PTEs in the soil using statistical analysis.

2. Materials and Methods

2.1. Study Area

The study area was located in the abandoned manganese mining area near Heling Town, Xiangtan City, Hunan Province, China (111°58'~113°05' E, 27°21'~28°05' N) (Figure 1). The study area is about 38.4 km^2. The Xiangtan City region is in a humid subtropical monsoon climate zone. It is dry in the summer and autumn, and vulnerable to cold waves and high winds in winter and spring. The average temperature is 16.7–17.4 °C. Precipitation is high, but the seasonal distribution is uneven and the inter-annual variation is large. The annual precipitation is 1200–1500 mm [5,10,11]. The overall topographical characteristics of Xiangtan City presents a sharply undulating landscape

with a maximum height of 150 m ASL with highest areas to the north, west, and south, and low lying areas in the central region and to the east. The Xiangtan City region is rich in mineral resources with the Mn-mineral deposits that are dominated by sedimentary manganese carbonate and secondary manganese oxide ore, as well as some non-metallic minerals, such as limestone, dolomite, coal, and gypsum [12]. We previously demonstrated the significance of surface processes in other locations of the mining region from the dispersal by wind blow and surface run off of residues close to former mining extraction points [5] and extended the work to mixed land use areas close to smelting and mining areas where farming had developed post-closure, to assess the impact of residual materials on the significance of exposure through the food chain [11]. This study identifies a residential location in the region, with external exposure from a range of sources, including mineral processing operations to provide a case to identify potential health impact from surface materials through external exposure (inhalation, dermal contact) pathways.
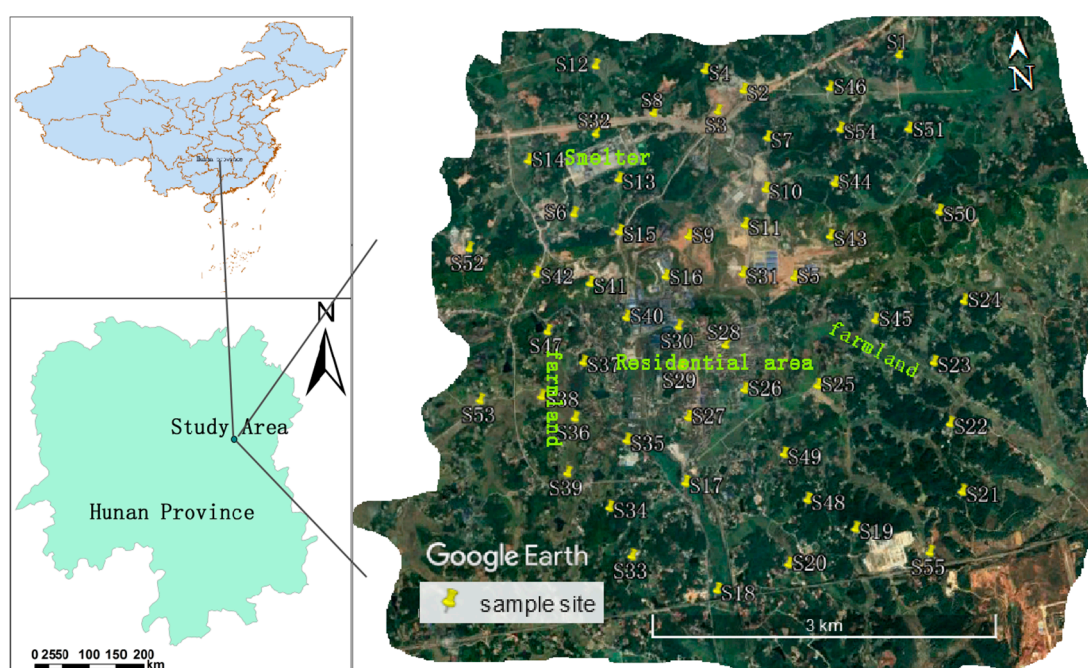

Figure 1. Distribution of sampling points in the study area.

2.2. Sample Collection

A total of 55 surface (0–20 cm) soil samples were collected in the study area between September and October 2018 (Figure 1). The samples were collected from the representative land uses to include agricultural soil, roadside soil, woodland soil, and disturbed soil near industrial operations. A total of five sub-samples were collected at each location based on a 5 m radius circle (points at east, west, south, north, and center) and mixed into a 1 kg composite sample [13]. The bulk samples were sealed in polyethylene bags and immediately sent to the laboratory. After removing the obvious debris such as wood chips, crushed stones, and animal and plant residues, the soil samples were air-dried at room temperature (20~25 °C), and then ground through a 200-mesh stainless steel sieve. The processed samples were packed in polyethylene bags, labeled, and stored in the refrigerator until they were analyzed [14].

2.3. Sample Analysis

The samples were digested with $HNO_3+HF+HClO_4$. Weighed 0.5 g of soil sample was placed in a Teflon beaker, and 15 mL $HNO_3+HF+HClO_4$ was added and digested at 85 °C until a clear solution was obtained [15]. It was then filtered through Whatman No.42 filter paper (<2.5 μm) and then diluted to 50 mL with deionized water. The concentration of Mn, Pb, Cu, Zn, Cr, Cd, and Ni were determined

by inductively coupled plasma mass spectrometry (ICP–MS, Finnigan MAT Element 2, ThermoFisher, Bremen DE). In sample detection, the limits were Mn (0.054 µg/kg), Pb (0.01 µg/kg), Cu (0.1 µg/kg), Zn (0.5 µg/kg), Cr (0.5 µg/kg), Cd (0.05 µg/kg), and Ni (0.03 µg/kg). In order to control the accuracy of the sample analysis, the standard reference material of the China National Standard Research Center (GBW07405-yellow/red soil, Hunan) was used and each sample was run as three replicates with reagent blanks monitored as controls. The recoveries for the target PTEs in GBW07405 were good and ranged between 95% and 104%.

3. Data Analysis

3.1. Geo-Accumulation Index (I_{geo})

The geo-accumulation index (I_{geo}) was first proposed by Muller [16] and is currently widely used to assess the level of metal pollution in soils and sediments. It is based on the comparison of the element content in the soil in the study area with the local background value. The formula used was:

$$I_{geo} = \log_2 \frac{C_n}{1.5C_r} \tag{1}$$

where C_n is the measured element concentration in the sample. C_r is the soil background value of the measured element. This study used the soil background value of Hunan Province [17]. The I_{geo} can be divided into seven categories, from less than 0 to greater than 5 (uncontaminated to extreme pollution) see (Table S1).

3.2. Pollution Load Index (PLI)

The pollution load index (PLI) was first proposed by Tomlinson et al. [18] in a screening tool for assessing the pollution level of trace elements. The results of PLI can reflect the enhanced contribution of PTEs to the substance load in the study area. The calculation formula is:

$$CF_n = \frac{C_n}{B_n} \tag{2}$$

$$PLI = \sqrt[n]{CF_1 \times CF_2 \times \cdots \times CF_n} \tag{3}$$

where CF_n is the pollution factor of element n. C_n is the content of element n in the sample. B_n is the background value of element n and this study used the soil background value of Hunan Province [17]. CF and PLI classifications are presented in Table S1.

3.3. Potential Ecological Risk Index (RI)

The potential ecological risk index (RI) was first proposed by Hakanson [19] in 1980. The RI assesses the ecological risk of PTEs in the soil based on element content and its toxicity [20]. The calculation formula is:

$$RI = \sum E_r^i = \sum T_r^i \times \left(\frac{C}{C_n^i} \right) \tag{4}$$

where RI is the sum of the potential ecological risks of various PTEs. E_r^i is the RI of an individual element. C is the content of PTEs in the sample. C_n^i is the background value of the element in the soil of Hunan Province. T_r^i is a toxic response factor of PTEs. The toxic response factors of Mn, Pb, Cu, Zn, Cr, Cd, and Ni are 1, 5, 5, 1, 2, 30, and 5, respectively [19,21,22]. The RI classification criteria for PTEs are found in the Supplementary Information (Table S2).

Int. J. Environ. Res. Public Health **2020**, *17*, 6554

5 of 15

3.4. Health Risk Assessment

The excessive ingestion of PTEs in the human body can cause acute or chronic health problems [23]. The hazard quotient (HQ) is widely used to study the health risks of adults and children in contaminated soil environments [24,25]. In addition, in order to assess the cumulative health risks generated by multiple elements, the HQ values of all PTEs are summed to obtain a comprehensive risk index, called the hazard index (HI) [26]. Carcinogenic risk (CR) is the probability that everyone will get cancer due to exposure to carcinogenic hazards. In the presence of multiple carcinogens, the total carcinogenic risk will increase with each carcinogen and exposure pathway [27,28]. The elements involved in carcinogenic risk in this study are Cr, Cd, and Ni. The calculation formulae for HQ, HI and CR are as follows:

$$HQ_{ingestion} = \frac{C \times IR \times RBA \times EF \times ED}{BW \times AT \times RfD_o} \times 10^{-6} \tag{5}$$

$$HQ_{dermal} = \frac{C \times SA \times AF_s \times ABS_d \times EF \times ED}{BW \times AT \times RfD_o \times GIABS} \times 10^{-6} \tag{6}$$

$$HQ_{inhalation} = \frac{C \times EF \times ED}{PEF \times AT \times RfC} \tag{7}$$

$$HI = \sum HQ \tag{8}$$

$$CR_{ingestion} = \frac{C \times IFS \times RBA \times CSF_o}{AT} \times 10^{-6} \tag{9}$$

$$IFS = \frac{EF \times ED(adult) \times IR(adult)}{BW(adult)} + \frac{EF \times ED(child) \times IR(child)}{BW(child)} \tag{10}$$

$$CR_{dermal} = \frac{C \times DFS \times ABS_d \times CSF_o}{AT \times GIABS} \times 10^{-6} \tag{11}$$

$$DFS = \frac{EF \times ED(adult) \times SA(adult) \times AF(adult)}{BW(adult)} + \frac{EF \times ED(child) \times SA(child) \times AF(child)}{BW(child)} \tag{12}$$

$$CR_{inhalation} = \frac{C \times EF \times ED \times IUR}{PEF \times AT} \times 10^3 \tag{13}$$

$$TCR = \sum CR \tag{14}$$

where C is the concentration (mg/kg). RBA (unitless) is the relative bioavailability factor (set to 1 according to USEPA) [29]. RfD_o (mg/kg·day) is based on USEPA non-carcinogenic risk oral reference dose [30]. ABS_d (unitless) is the dermal absorption rate, the value of which is determined by USEPA [24]. GIABS (unitless) is a gastrointestinal absorption factor, the value of which is determined by USEPA [30]. PEF (m^3/kg) is a particulate emission factor, the value of which is determined by USEPA [30]. RfC (mg/m^3) is the inhalation reference concentration, the value of which is determined by USEPA [30]. IFS (mg/kg) is the soil ingestion ratio, the specific value of which is determined by the formula, which is derived from USEPA [29]. DFS (mg/kg) is the soil dermal contact factor, the specific value is determined by the formula, which is derived from USEPA [29]. IUR ($(\mu g/m^3)^{-1}$) is the inhalation unit risk, the value of which is determined by USEPA [30]. The definition and values of the parameters in the formula are provided in the Supplementary Information (Tables S3 and S4).

When HQ (HI) < 1, it is generally considered health protective. In contrast, when HQ (HI) > 1, and increased health risk may occur, which increases as the HQ (HI) value becomes higher [31]. Similarly, when CR < 10^{-6}, there is negligible carcinogenic risk; when 10^{-6} < CR < 10^{-4}, there may be carcinogenic risk, but it is acceptable; and when CR > 10^{-4}, there is a high carcinogenic risk.

3.5. Statistical Analysis

Descriptive statistical analysis of soil properties and PTE content was performed using SPSS22 (IBM, Armonk, NY, USA). The Pearson correlation coefficient matrix and PCA were used to identify the source of PTEs. In addition, they can provide effective information to identify the source of elements in the study area [1,32]. Origin9 was used to convert the data into graphics, making the assessment more intuitive. Kriging interpolation in ArcGIS 10.3 (ESRI, Redlands, CA, USA) can be used to obtain the information relating to the spatial distribution of PTEs.

4. Results and Discussion

4.1. Pollution and Spatial Distribution of PTEs

4.1.1. Pollution Significance

The average concentrations of Mn, Pb, Cu, Zn, Cr, Cd, and Ni in the soil were 1876.67, 40.76, 45.03, 105.07, 41.24, 0.54, and 30.94 mg/kg, respectively (Table 1), exceeding the background values of these elements in Hunan Province by 4.09, 1.37, 1.65, 1.1, 0.58, 4.29, and 0.97 times, respectively. The coefficient of variation (CV) can reveal the disturbance of the soil properties by inputs from the external environment or natural heterogeneity. In general, the higher the CV value, the more severe the disruption [33]. In this study, the high average concentration, the extreme maximum values and high CV for Mn, Pb, Cu, Zn, and Cd indicate that this area might be impacted by external factors such as anthropogenic interference from mining and traffic-derived emissions.

Table 1. Potentially toxic elements (PTEs) concentrations and descriptive statistics in the soil (mg/kg).

Element	Minimum	Maximum	Mean ± SD	CV (%)	Background Values	I_{geo}
Mn	1005.70	4247.49	1877.67 ± 685.01	36.5	459	1.37
Pb	21.48	87.10	40.76 ± 15.52	38.1	29.7	−0.21
Cu	17.73	96.26	45.03 ± 16.17	35.9	27.3	0.05
Zn	49.08	268.75	105.07 ± 50.73	48.3	94.4	−0.56
Cr	26.34	54.50	41.24 ± 6.81	16.5	71.4	−1.40
Cd	0.12	0.86	0.54 ± 0.17	31.5	0.126	1.40
Ni	21.79	39.57	30.94 ± 5.20	16.8	31.9	−0.65

SD: standard deviation; Geo-accumulation index (I_{geo}) is the mean value, CV (%) coefficient of variation.

The concentrations of the PTEs in the soil descended in the order Mn > Zn > Pb > Cu > Cr > Ni > Cd. Comparing this to the soil background values for Hunan Province [17], the percentage of samples with contents of Mn, Pb, Cu, Zn, Cr, Cd, and Ni exceeding their background values were 100%, 81.8%, 89.1%, 43.6%, 0%, 98.2%, and 47.3%, respectively. However, compared with other regions in China, Pb, Cu, Zn, Cr, and Cd in this region were lower than those for example from the thallium mining area of Guizhou [1]. For Pb, Zn, Cr, and Cd, the soil contents in this region were lower than that found in the copper mining area of Henan [34]. Apart from Mn, all other elements in this region were lower than for those in the Dexing Copper mining area of Jiangxi [35]. Compared with other mining areas internationally, such as the Malaysian bauxite mining areas, all elements in this region were higher [36]. Compared with the Nigerian Pb–Zn mining regions, Mn, Cu, Cr, and Ni in this region were at higher concentrations, while Pb, Zn, and Cd were at lower concentrations [37] and compared to an India chromite mining area, all elements except Cr and Ni were at higher concentrations [38] (Table 2). The region therefore shows modest levels of contamination by mining derived emissions and the samples collected in this campaign showing significantly lower levels than those from our study closer to mining and smelting operations in other parts of the region [5].

Table 2. Concentrations of soil PTEs (mg/kg) in abandoned manganese mines and other areas in Xiangtan.

	Mn	Pb	Cu	Zn	Cr	Cd	Ni	References
Xiangtan abandoned manganese mine area	1877.65	40.76	45.03	105.07	41.24	0.54	30.94	This study
Guizhou thallium mining area	-	44.39	79.63	118.23	52.11	1.14	-	Jiang et al. [1]
Henan coal mining area	-	70.10	26.97	109.63	50.97	0.61	-	Li et al. [34]
Dexing mining area in Jiangxi	-	98.6	65	134	77.8	1.3	35.9	Lin et al. [35]
Malaysia bauxite mining areas	192.42	13.70	10.73	44.01	34.25	0.13	-	Kusin et al. [36]
Nigeria Pb–Zn mining	788.14	132.4	18.19	134	40.71	0.6	22.23	Obiora et al. [37]
India chromite mining area	-	11.28	24.00	98.54	499.94	-	168.49	Krishna et al. [38]

4.1.2. Spatial Distribution

In ArcGIS 10.3 (ESRI, Redlands, CA, USA), Kriging interpolation was used to obtain the visual information of the spatial distribution of the seven PTEs (Figure 2). The maximum concentrations of Mn, Pb, Cu, and Zn were all located in the northwest of the study area. Cd was at a high concentration in the south and Cr and Ni were at a high concentration in the southwest (Figure 2). The results of the field investigations revealed that the entire research area was affected by the legacy of direct mining and the impact of smelting and transportation. Frequent mining activities, smelting and transportation may cause changes in the concentration of Mn and other PTEs. In addition, agricultural activities and municipal wastewater production may also interfere with the distribution of Cd and other PTEs in this study area. A large number of herbicides and pesticides used by residents in agricultural activities will also increase the Cd concentration in the soil, and agricultural activities will change soil migration properties. The variation of Cr and Ni was low throughout the study area, and the concentration of Cr was less than the background value, with Ni fluctuating around the background value, indicating that these two elements were likely to be subject to only minor inputs from anthropogenic activity.
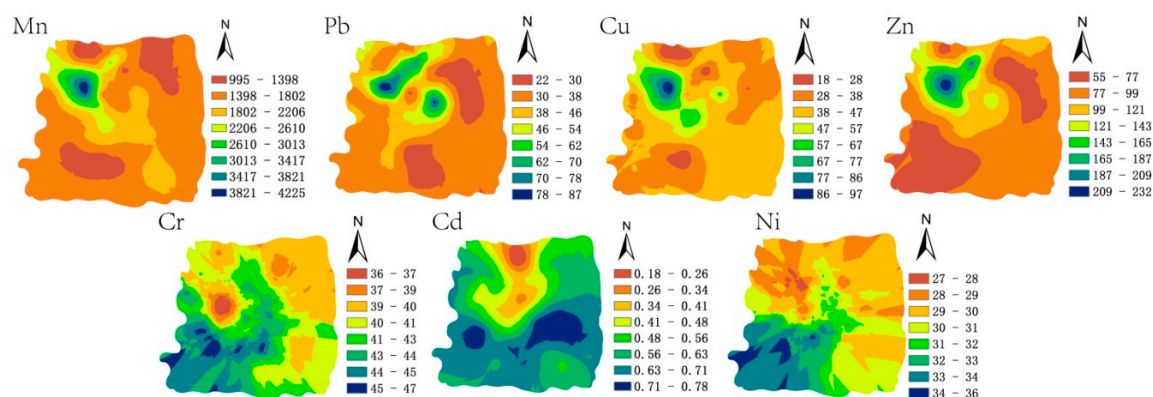
Figure 2. PTE concentration (mg/kg) distribution in the soil of the study area.

4.2. Environmental Risk Assessment

4.2.1. Geo-Accumulation Index (I_{geo})

The calculation results showed that the ranges of I_{geo} were from 0.55 to 2.63, −1.05 to 0.97, −1.21 to 1.23, −1.53 to 0.92, −2.02 to −0.97, −0.66 to 2.19, and −1.13 to −0.27 for Mn, Pb, Cu, Zn, Cr, Cd, and Ni, respectively (Figure 3). The average I_{geo} values were −1.40, −0.65, −0.56, and −0.21 for Cr, Ni, Zn, and Pb, respectively (Table 1), and the I_{geo} of all the sampling points were lower than 0 for Cr and Ni, and for Zn and Pb, over 70% of the sampling sites were below 0 (Table S5), so Cr, Ni, Zn, and Pb were uncontaminated in the study area. The average I_{geo} of Cu was 0. 05 and the I_{geo} values for 47.3% of the sampling points were less than 0, and 47.2% of the sampling points were less than 1 (Table S5). Therefore, the Cu data were generally assessed to be at an uncontaminated to moderate contamination level. The average I_{geo} was 1.37 and 1.40 for Mn and Cd, respectively,

and more than 70% of the sampling points were classified to be at moderate contamination levels (Table S5). Therefore, the pollution situation in the entire study area reflects a moderate contamination highlighting the potential need for remediation measures to be made.
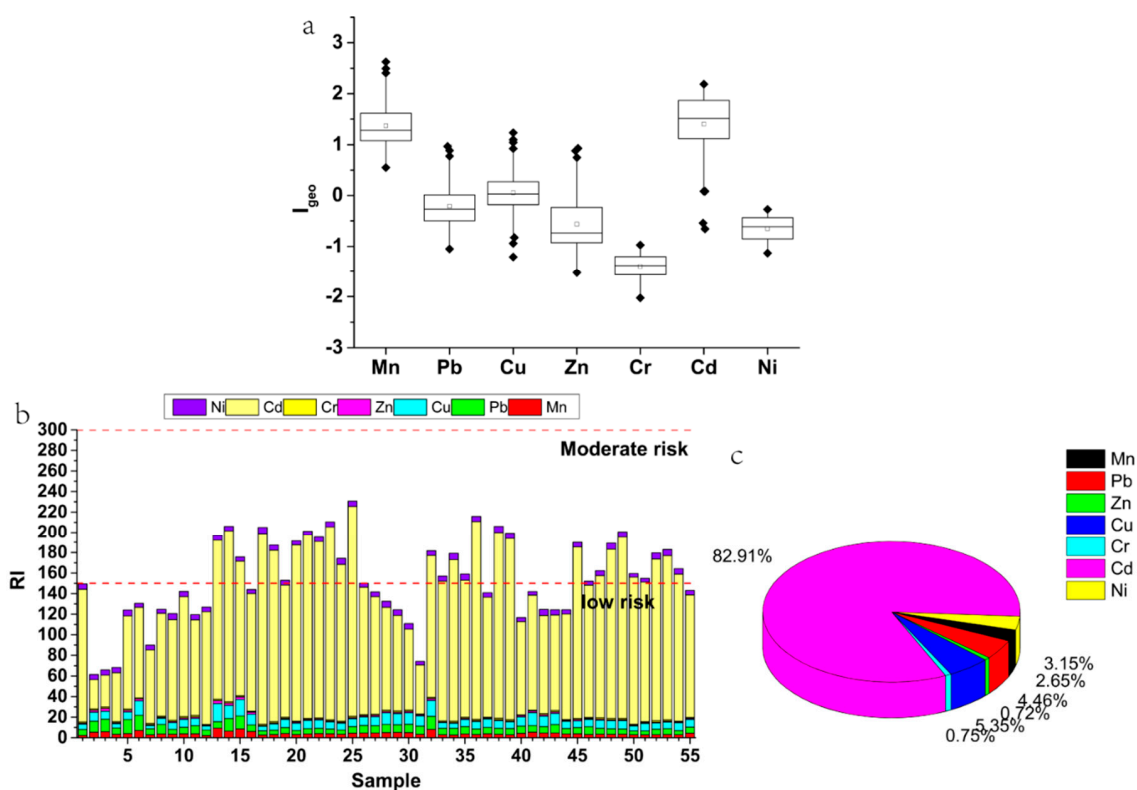

Figure 3. Contribution of the I_{geo} (**a**), potential ecological risk index (RI) of PTEs (**b**) and the E_r^i of various elements to RI (**c**) in the soil of the study area.

4.2.2. Pollution Load Index (PLI)

The results of the PLI calculation for PTEs in the soil samples are shown in the Supplementary Information (Figure S1). The range of CF values were 2.19–9.25, 0.72–2.93, 0.65–3.53, 0.52–2.85, 0.37–0.76, 0.95–6.83, and 0.68–1.24 for Mn, Pb, Cu, Zn, Cr, Cd, and Ni, respectively. In addition, the order of average CF for these PTEs was Cd > Mn > Cu > Pb > Zn > Ni > Cr. This indicates that due to human disturbance, the introduction and distribution of these PTEs in the soil are different [39]. According to the PLI classification standard, 92.7% of the sampling points were in the moderate contamination category, and 7.3% of the sampling points were in the considerable contamination category, confirming the result from the calculation of I_{geo}.

4.2.3. Potential Ecological Risk Index (RI)

Figure 3 and Table S5 show the results of the E_r^i and RI calculations for the PTEs in the soil samples. The ecological risks were lower for Mn, Pb, Cu, Zn, Cr, and Ni than for Cd (Figure 3b). Apart for Cd, the maximum and average values were lower than 40 for the E_r^i for the elements concerned, indicating that the sampling locations are at low ecological risk across the study area. The average E_r^i of Cd was 127.79, and the maximum value was more than 200, indicating that there is a potentially significant ecological risk. This may be related to the low background value of Cd in Hunan Province and the high toxic response factor of Cd (30). The range and average of RI were 61.43–230.67 and 154.13, respectively, where, 45.5% were at low risk and 54.5% were at medium risk. Compared with other studies, the average values of PI in the Henan copper mining area and Malaysia bauxite mining areas were 244.4 and 44.93, respectively [34,36]. Therefore, the region as a whole is at a moderate ecological

risk. Figure 3 also revealed the contribution of various elements to RI. With Cd dominating through a 82.91% contribution to the RI, followed by Cu and Pb, which contributed 5.35% and 4.46%, respectively, the need for Cd to be prioritized is highlighted as found in previous studies [3,34].

4.3. Source Analysis

Pearson correlation coefficient matrix, PCA and rotated component matrix have been widely used to determine the source of PTEs in the soil [1,40,41]. The results of the Pearson correlation coefficient matrix reflected the complex relationship between PTEs in the soil samples (Table 3). The correlations between Mn, Pb, Cu, and Zn were strong ($r^2 > 0.5$), and Cr and Ni were also strongly correlated ($r^2 = 0.761$). However, the correlation between Cd and other elements was low. Strong correlation indicates that these elements may have common sources, similar migration behavior and pathways in the study area [1,42,43].

Table 3. Pearson correlation coefficient matrix between PTEs in the soil.

	Mn	Pb	Cu	Zn	Cr	Cd	Ni
Mn	1						
Pb	0.642 **	1					
Cu	0.912 **	0.550 **	1				
Zn	0.874 **	0.694 **	0.731 **	1			
Cr	−0.044	0.018	−0.057	0.003	1		
Cd	−0.183	−0.451 **	−0.099	−0.344 *	0.230	1	
Ni	−0.227	−0.131	−0.241	−0.175	0.761 **	0.183	1

** indicates that the correlation reached a significant level of 0.01 (two-tailed), * indicates that the correlation reached a significant level of 0.05 (two-tailed).

Kaiser–Meyer–Olkin (KMO) and Bartlett's spherical tests were performed on the data before the PCA analysis of the PTE content in the soil. The KMO value of the PTEs in the soil was 0.673, and the Bartlett's spherical test value was 275.48 (df = 21, Sig = 0.000 < 0.001), indicating that the data were suitable for PCA in this study [44]. Three principal components (PCs) (eigenvalues > 1) were obtained from the data for the seven PTEs in the soil samples, explaining almost 88% of the data variability. According to the rotation component matrix and loading diagram (Table 4 and Figure S2), the first principal component (PC1) accounted for ~49% of the total variance, of which high load elements were Mn, Pb, Cu, and Zn. According to field investigations, high concentrations of Mn, Cu, and Zn may be directly derived from manganese ore activities (such as mining, smelting, and tailing deposits) [45]. In addition, Cu may also originate from the wear of tires and brake linings of vehicles. The main source of Pb is likely to be historical emissions from the use of leaded gasoline by traffic [46]. Although China banned the use of leaded gasoline since 2000, recent reports still show elevated Pb in roadside soil [47]. Although the mining areas in the region have ceased production, the effects of mining, smelting, and tailings on soil for many years still exist. In addition, the strong correlations between Mn, Pb, Cu, and Zn and the similar spatial distribution of these elements also indicate that these elements had a common source (Figure 2 and Table 3). Therefore, the first principal component (PC1) can be considered to be derived from mining activities and related transportation emissions.

Int. J. Environ. Res. Public Health **2020**, *17*, 6554

10 of 15

Table 4. Total variance and principal component analysis (PCA) of PTEs concentrations in the soil. Strong contribution of components to variability in individual PCs highlighted in **bold**.

Component	Initial Eigenvalues			Element	Rotated Component		
	Total	% of Variance	Cumulative %		PC1	PC2	PC3
1	3.341	49.008	49.008	Mn	**0.974**	−0.075	0.046
2	1.738	24.830	73.838	Pb	**0.739**	0.057	−0.466
3	1.018	14.538	88.377	Cu	**0.922**	−0.110	0.166
4	0.344	4.917	93.294	Zn	**0.909**	−0.001	−0.192
5	0.220	3.145	96.438	Cr	0.034	**0.941**	0.111
6	0.201	2.878	99.317	Cd	−0.192	0.156	**0.930**
7	0.048	0.683	100.000	Ni	−0.187	**0.922**	0.019

The second principal component (PC2) accounted for 24.8% of the total variance, where Cr and Ni had high loadings. The sources of Cr and Ni are commonly natural weathering, industrial (electroplate or tannery), and tailings deposits from manganese mining area [48,49]. According to field investigations, there was no electroplating and tannery industry in the study area, although the concentration of Ni at some sampling points was higher than the soil background value in Hunan Province. In this study, overall, the Ni content fluctuated around the soil background value of Hunan Province and the average value was lower than the background value of Hunan Province. The Cr content was lower than the background value for Hunan Province across the whole study area. In addition, the CV were 16.5% and 16.8% for Cr and Ni, respectively, both of which were lower than 30%, indicating that these two elements were less affected by human interference. Combined with the results from the Pearson correlation coefficient matrix, where Cr and Ni have a strong correlation, this indicates that they are likely to have a common source. Therefore, PC2 can be considered to be dominated by natural inputs.

The third principal component (PC3) accounted for 14.5% of the total variance, for which Cd had a high loading. The Cd may have derived from municipal sewage discharge, agricultural production, and atmospheric deposition [50]. The presence of Cd, as an additive, is widely used in pesticides and is well known locally as a natural contaminant in phosphate fertilizers [51,52]. In this study, samples with higher Cd concentrations were from agricultural areas and towns in the south of the study area. Combined with the Pearson correlation coefficient matrix, the correlation between Cd and several other elements was very low, indicating that Cd is different from other elements. Therefore, PC3 can be considered to be derived from agricultural production and municipal sewage discharge.

4.4. Health Risk Assessment

4.4.1. Non-Carcinogenic Risk

The non-carcinogenic risk analysis for soil sampling sites in the study area for adults and children under different exposure routes is shown in Figure 4 (and Table S6). For adults and children, the relationship between the average non-carcinogenic risk of PTEs in soil was Mn > Pb > Cr > Ni > Cu > Cd > Zn (Table S6). The HQ for all elements was less than one, indicating that these elements do not pose a health risk (Table S6). Similarly, the average values of total HI were 0.215 and 0.905 for adults and children, respectively, which were both lower than one. It shows that there is low toxicity risk across the study area. However, for children, the HI value at some locations was higher than unity, (23.6% of the total sampling points). This shows that whilst overall the region does not present a significant non-carcinogenic risk, this is not uniform and some locations may show significant non-carcinogenic risks for children. These sampling points are mostly located near factories in the north and in urban areas. In addition, Mn has the highest contribution to the total HI, accounting for 76.3% and 73.9% for adult and children, respectively. Figure 4 shows the significant difference between the health risk from PTEs in the soil for adults compared to children, agreeing with previous studies [1,9,53,54].

In addition, the contribution of the three exposure routes to total HI was $HQ_{ing} > HQ_{inh} > HQ_{der}$ (adult), $HQ_{ing} > HQ_{der} > HQ_{inh}$ (child), where, HQ_{ing} accounted for 79.8% (adults) and 90.9% (children) of total HI, respectively.
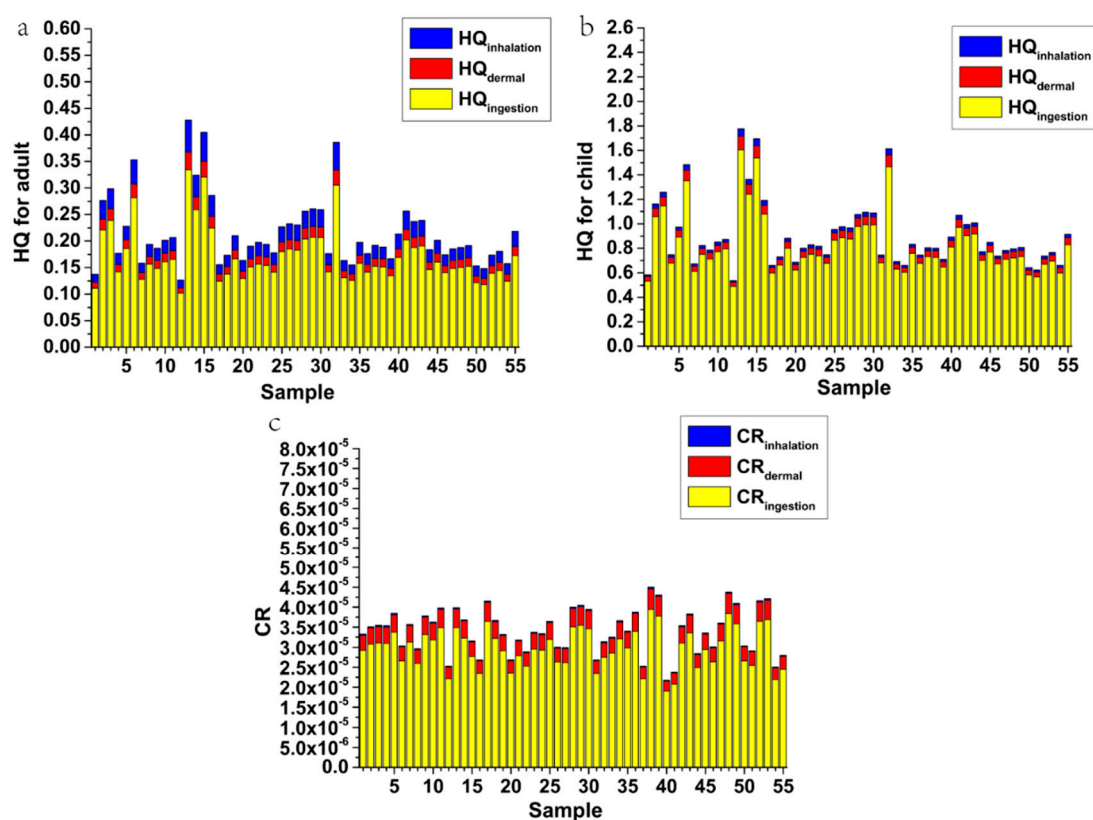

Figure 4. Non-carcinogenic ((**a**): adult and (**b**): child) and carcinogenic risks (CRs) (**c**) of PTEs in soil.

4.4.2. Carcinogenic Risk

The carcinogenic risk analysis for adults and children under different exposure routes is shown in Figure 4 (and Table S6). The average of the total carcinogenic risk was 3.40×10^{-5} for Cr, Cd, and Ni (Table S7). This indicates that the study area may have an increased carcinogenic risk, but it is acceptable. The relationship between the carcinogenic risk of the three exposure routes was $CR_{ing} > CR_{der} > CR_{inh}$ (Figure 4). Therefore, the ingestion route is the main source of carcinogenic risk, accounting for 87.7% of the total carcinogenic risk, dermal contact accounts for 11.5% of the total carcinogenic risk and the contribution of inhalation was insignificant.

4.5. Practical Implications of This Study

In this study, the soil from the abandoned manganese ore area in Xiangtan evaluated by I_{geo}, PLI, RI, HQ, HI and CR and statisical assessment using PCA and Pearson correlation coefficient. The results highlighted the significance of a number of human inputs which can be used, combined with spatial analysis, to drive the further management of the abandoned region as it is redeveloped., and also be used to analyze the source of soil pollution. According to these results, we can understand the soil pollution in the study area. In the future, the soil will be treated according to its condition, so that it can be re-used better.

Int. J. Environ. Res. Public Health **2020**, *17*, 6554

12 of 15

5. Conclusions

From the assessment of soil contamination in the abandoned mining area:

1. The relationship between the concentration of seven PTEs in the soil system was Mn > Zn > Pb > Cu > Cr > Ni > Cd, where, the concentrations of Mn and Cd, respectively, exceeded their background values by four times. The high average concentration, extreme maximum, and high CV for Mn, Pb, Cu, Zn, and Cd indicate that they have been affected by external sources such as anthropogenic interference (mining and transportation emissions).

The spatial distribution of PTEs showed the north of the region with the most significant concentrations. Calculations of I$_{geo}$, PLI, and RI indicate that across the entire study area, a moderate level of pollution but with some spatial variation including significant peaks.

2. The results of the statistical analysis (Pearson correlation coefficient and PCA) show that PTEs in the survey area are influenced by three discrete sources: mining activity and associated material movement (Mn, Pb, Cu, and Zn), natural geological background (Cr and Ni), and agriculture/municipal waste water (Cd).

3. From the health risk assessment, the non-carcinogenic risk was negligible (HI < 1) across the entire study area, but for children, some locations showed an enhanced risk HI > 1. The HI values for children were significantly higher than for the adults and for the three exposure routes of ingestion, dermal contact, and inhalation, ingestion was the most important. The evaluation of carcinogenic risk showed that there is an acceptable carcinogenic risk and that ingestion was also the main exposure route for carcinogenic risk.

Supplementary Materials: The following are available online at http://www.mdpi.com/1660-4601/17/18/6554/s1, Figure S1: The contamination factors and pollution load index of PTEs in soil, Figure S2: Load diagram in rotating space, Table S1: Levels of I$_{geo}$, CF and PLI; Table S2: Potential ecological risk index classification standard; Table S3: Exposure factors used in estimation for non-carcinogenic risk and carcinogenic risk; Table S4: Some parameter values of various PTEs; Table S5: The distribution of I$_{geo}$ and E$_r^i$ of PTEs at each level, Table S6: Non-carcinogenic risk hazard quotient (HQ) and risk index (HI), Table S7: Carcinogenic risk under exposure pathways.

References

1. Jiang, F.; Ren, B.; Hursthouse, A.; Deng, R.; Wang, Z. Distribution, source identification, and ecological-health risks of potentially toxic elements (PTEs) in soil of thallium mine area (southwestern Guizhou, China). *Environ. Sci. Pollut. Res. Int.* **2019**, *26*, 16556–16567. [CrossRef]

2. Wu, W.; Wu, P.; Yang, F.; Sun, D.L.; Zhang, D.X.; Zhou, Y.K. Assessment of heavy metal pollution and human health risks in urban soils around an electronics manufacturing facility. *Sci. Total Environ.* **2018**, *630*, 53–61. [CrossRef] [PubMed]

3. Zheng, L.; Zhou, Z.; Rao, M.; Sun, Z. Assessment of heavy metals and arsenic pollution in surface sediments from rivers around a uranium mining area in East China. *Environ. Geochem. Health* **2020**, *42*, 1401–1413. [CrossRef]

4. El Azhari, A.; Rhoujjati, A.; El Hachimi, M.L.; Ambrosi, J.-P. Pollution and ecological risk assessment of heavy metals in the soil-plant system and the sediment-water column around a former Pb/Zn-mining area in NE Morocco. *Ecotoxicol. Environ. Saf.* **2017**, *144*, 464–474. [CrossRef]

5. Jiang, F.; Ren, B.; Hursthouse, A.S.; Zhou, Y. Trace metal pollution in topsoil surrounding the Xiangtan manganese mine area (south-central China): Source identification, spatial distribution and assessment of potential ecological risks. *Int. J. Environ. Res. Public Health* **2018**, *15*, 2412. [CrossRef] [PubMed]

6.   Li, Y.; Yang, X.; Bing, G.; Xue, L. Effective bioremediation of Cu(II) contaminated waters with immobilized sulfate-reducing bacteria-microalgae beads in a continuous treatment system and mechanism analysis. *J. Chem. Technol. Biotechnol.* **2018**, *93*, 1453–1461. [CrossRef]

7.   Pareja-Carrera, J.; Mateo, R.; Rodriguez-Estival, J. Lead (Pb) in sheep exposed to mining pollution: Implications for animal and human health. *Ecotoxicol. Environ. Saf.* **2014**, *108*, 210–216. [CrossRef]

8.   Sawut, R.; Kasim, N.; Maihemuti, B.; Hu, L.; Abliz, A.; Abdujappar, A.; Kurban, M. Pollution characteristics and health risk assessment of heavy metals in the vegetable bases of northwest China. *Sci. Total Environ.* **2018**, *642*, 864–878. [CrossRef]

9.   Tepanosyan, G.; Sahakyan, L.; Belyaeva, O.; Maghakyan, N.; Saghatelyan, A. Human health risk assessment and riskiest heavy metal origin identification in urban soils of Yerevan, Armenia. *Chemosphere* **2017**, *184*, 1230–1240. [CrossRef] [PubMed]

10. Fang, X.; Tian, D.L.; Xie, R.X. Soil physical and chemical properties of the wasteland in Xiangtan manganese mine. *Acta Ecol. Sin.* **2006**, *26*, 1494–1501.

11. Luo, X.; Ren, B.; Hursthouse, A.S.; Jiang, F.; Deng, R.J. Potentially toxic elements (PTEs) in crops, soil, and water near Xiangtan manganese mine, China: Potential risk to health in the foodchain. *Environ. Geochem. Health* **2019**, *42*, 1965–1976. [CrossRef] [PubMed]

12. Yan, W.; Xiang, J.; Tian, D. Study on soil properties of waste land in Xiangtan mining industry, Hunan Province. *Sci. Silvae Sin.* **2006**, *42*, 12–18.

13. Ji, K.; Kim, J.; Lee, M.; Park, S.; Kwon, H.J.; Cheong, H.K.; Jang, J.Y.; Kim, D.S.; Yu, S.; Kim, Y.W.; et al. Assessment of exposure to heavy metals and health risks among residents near abandoned metal mines in Goseong, Korea. *Environ. Pollut.* **2013**, *178*, 322–328. [CrossRef] [PubMed]

14. Li, Q.; Chen, Y.; Fu, H.; Cui, Z.; Shi, L.; Wang, L.; Liu, Z. Health risk of heavy metals in food crops grown on reclaimed tidal flat soil in the Pearl River Estuary, China. *J. Hazard. Mater.* **2012**, *227*, 148–154. [CrossRef] [PubMed]

15. Lian, M.; Wang, J.; Sun, L.; Xu, Z.; Tang, J.; Yan, J.; Zeng, X. Profiles and potential health risks of heavy metals in soil and crops from the watershed of Xi River in Northeast China. *Ecotoxicol. Environ. Saf.* **2019**, *169*, 442–448. [CrossRef]

16. Muller, G. Index of geoaccumulation in sediments of the Rhine River. *Geojournal* **1969**, *2*, 108–118.

17. CEME. *The Background Values of Chinese Soils, China Environmental Monitoring Center*; Chinese Environment Science Press: Beijing, China, 1990.

18. Tomlinson, D.L.; Wilson, J.G.; Harris, C.R.; Jeffrey, D.W. Problems in the assessment of heavy-metal levels in estuaries and the formation of a pollution index. *Helgoländer Meeresunters* **1980**, *33*, 566–575. [CrossRef]

19. Hakanson, L. An ecological risk index for aquatic pollution control.a sedimentological approach. *Water Res.* **1980**, *14*, 975–1001. [CrossRef]

20. Wu, J.; Lu, J.; Li, L.; Min, X.; Luo, Y. Pollution, ecological-health risks, and sources of heavy metals in soil of the northeastern Qinghai-Tibet Plateau. *Chemosphere* **2018**, *201*, 234–242. [CrossRef]

21. Xu, Z.Q.; Ni, S.J.; Tuo, X.G.; Zhang, C.J. Calculation of heavy metals' toxicity coefficient in the evaluation of potential ecological risk index. *Environ. Sci. Technol.* **2008**, *31*, 112–115.

22. Ahmed, I.; Mostefa, B.; Bernard, A.; Olivier, R. Levels and ecological risk assessment of heavy metals in surface sediments of fishing grounds along Algerian coast. *Mar. Pollut. Bull.* **2018**, *136*, 322–333. [CrossRef] [PubMed]

23. Yang, Y.; Xiao-Song, L.U.; Ding-Long, L.I. Research progress of environmental health risk assessment in China. *J. Environ. Health* **2014**, *31*, 357–361.

24. USEPA. *Risk Assessment Guidance for Superfund Volume I Human Health Evaluation Manual (Part. E, Supplemental Guidance for Dermal Risk Assessment)*; EPA/540/R/99/005; Office of Superfund Remediation and Technology Innovation U.S. Environmental Protection Agency: Washington, DC, USA, 2004.

25. USEPA. *Exposure Factors Handbook: Volume I-General Factors*; Office of Superfund Remediation and Technology Innovation U.S. Environmental Protection Agency: Washington, DC, USA, 2000.

26. USEPA. Guidelines for the health risk assessment of chemical mixtures. *Fed. Reg.* **1986**, *51*, 34014–34025.

27. Li, Z.; Ma, Z.; van der Kuijp, T.J.; Yuan, Z.; Huang, L. A review of soil heavy metal pollution from mines in China: Pollution and health risk assessment. *Sci. Total Environ.* **2014**, *468*, 843–853. [CrossRef] [PubMed]

28. USEPA. *Guidelines for Carcinogen Risk Assessment*; Risk Assessment Forum US Environmental Protection Agency: Washington, DC, USA, 2005.

29. USEPA. Regional Screening Levels (RSLs)-User's Guide pdf. Available online: https://www.epa.gov/risk/regional-screening-levels-rsls-users-guide#main-content (accessed on 20 August 2020).

30. USEPA. Risk-Based Concentration Table. Available online: http://www.epa.gov/region9/superfund/prg/ (accessed on 20 August 2020).

31. Cao, S.; Duan, X.; Zhao, X.; Ma, J.; Dong, T.; Huang, N.; Sun, C.; He, B.; Wei, F. Health risks from the exposure of children to As, Se, Pb and other heavy metals near the largest coking plant in China. *Sci. Total Environ.* **2014**, *472*, 1001–1009. [CrossRef] [PubMed]

32. Manta, D.S.; Angelone, M.; Bellanca, A.; Neri, R.; Sprovieri, M. Heavy metals in urban soils: A case study from the city of Palermo (Sicily), Italy. *Sci. Total Environ.* **2002**, *300*, 229–243. [CrossRef]

33. Zhao, K.; Liu, X.; Xu, J.; Selim, H.M. Heavy metal contaminations in a soil-rice system: Identification of spatial dependence in relation to soil properties of paddy fields. *J. Hazard. Mater.* **2010**, *181*, 778–787. [CrossRef]

34. Li, K.; Gu, Y.; Li, M.; Zhao, L.; Ding, J.; Lun, Z.; Tian, W. Spatial analysis, source identification and risk assessment of heavy metals in a coal mining area in Henan, Central China. *Int. Biodeterior. Biodegrad.* **2018**, *128*, 148–154. [CrossRef]

35. Lin, W.; Wu, K.; Lao, Z.; Hu, W.; Lin, B.; Li, Y.; Fan, H.; Hu, J. Assessment of trace metal contamination and ecological risk in the forest ecosystem of dexing mining area in northeast Jiangxi Province, China. *Ecotoxicol. Environ. Saf.* **2019**, *167*, 76–82. [CrossRef]

36. Kusin, F.M.; Azani, N.N.M.; Hasan, S.N.M.S.; Sulong, N.A. Distribution of heavy metals and metalloid in surface sediments of heavily-mined area for bauxite ore in Pengerang, Malaysia and associated risk assessment. *Catena* **2018**, *165*, 454–464. [CrossRef]

37. Obiora, S.C.; Chukwu, A.; Davies, T.C. Heavy metals and health risk assessment of arable soils and food crops around Pb–Zn mining localities in Enyigba, southeastern Nigeria. *J. Afr. Earth Sci.* **2016**, *116*, 182–189. [CrossRef]

38. Krishna, A.K.; Mohan, K.R.; Murthy, N.N.; Periasamy, V.; Bipinkumar, G.; Manohar, K.; Rao, S.S. Assessment of heavy metal contamination in soils around chromite mining areas, Nuggihalli, Karnataka, India. *Environ. Earth Sci.* **2013**, *70*, 699–708. [CrossRef]

39. Pang, S.; Ting-Xuan, L.I.; Wang, Y.D.; Hai-Ying, Y.U.; Guo, Q.L.; Chen, D.M. Spatial variability and influencing factors of the concentrations of Cu, Zn, and Cr in cropland soil on county scales. *Sci. Agric. Sin.* **2010**, *43*, 737–743.

40. Al-Khashman, O.A.; Shawabkeh, R.A. Metals distribution in soils around the cement factory in southern Jordan. *Environ. Pollut.* **2006**, *140*, 387–394. [CrossRef] [PubMed]

41. Acosta, J.A.; Gabarron, M.; Faz, A.; Martinez-Martinez, S.; Zornoza, R.; Arocena, J.M. Influence of population density on the concentration and speciation of metals in the soil and street dust from urban areas. *Chemosphere* **2015**, *134*, 328–337. [CrossRef] [PubMed]

42. Li, X.; Yang, H.; Zhang, C.; Zeng, G.; Liu, Y.; Xu, W.; Wu, Y.; Lan, S. Spatial distribution and transport characteristics of heavy metals around an antimony mine area in central China. *Chemosphere* **2017**, *170*, 17–24. [CrossRef]

43. Wang, Y.; Hu, J.; Xiong, K.; Huang, X.; Duan, S. Distribution of heavy metals in core sediments from Baihua Lake. *Procedia Environ. Sci.* **2012**, *16*, 51–58. [CrossRef]

44. Varol, M. Assessment of heavy metal contamination in sediments of the Tigris River (Turkey) using pollution indices and multivariate statistical techniques. *J. Hazard. Mater.* **2011**, *195*, 355–364. [CrossRef]

45. Liang, J.; Liu, J.; Yuan, X.; Zeng, G.; Yuan, Y.; Wu, H.; Li, F. A method for heavy metal exposure risk assessment to migratory herbivorous birds and identification of priority pollutants/areas in wetlands. *Environ. Sci. Pollut. Res. Int.* **2016**, *23*, 11806–11813. [CrossRef]

46. Yang, Z.; Zhang, Z.; Chai, L.; Wang, Y.; Liu, Y.; Xiao, R. Bioleaching remediation of heavy metal-contaminated soils using Burkholderia sp. Z-90. *J. Hazard. Mater.* **2016**, *301*, 145. [CrossRef]

47. Yan, G.; Mao, L.; Liu, S.; Mao, Y.; Ye, H.; Huang, T.; Li, F.; Chen, L. Enrichment and sources of trace metals in roadside soils in Shanghai, China: A case study of two urban/rural roads. *Sci. Total. Environ.* **2018**, *631*, 942–950. [CrossRef] [PubMed]

48. Lv, J.; Liu, Y.; Zhang, Z.; Dai, B. Multivariate geostatistical analyses of heavy metals in soils: Spatial multi-scale variations in Wulian, Eastern China. *Ecotoxicol. Environ. Saf.* **2014**, *107*, 140–147. [CrossRef] [PubMed]

49. Sun, C.; Liu, J.; Wang, Y.; Sun, L.; Yu, H. Multivariate and geostatistical analyses of the spatial distribution and sources of heavy metals in agricultural soil in Dehui, Northeast China. *Chemosphere* **2013**, *92*, 517–523. [CrossRef] [PubMed]

50. Rehman, M.Z.U.; Rizwan, M.; Hussain, A.; Saqib, M.; Ali, S.; Sohail, M.I.; Shafiq, M.; Hafeez, F. Alleviation of cadmium (Cd) toxicity and minimizing its uptake in wheat (triticum aestivum) by using organic carbon sources in Cd-spiked soil. *Environ. Pollut.* **2018**, *241*, 557–565. [CrossRef] [PubMed]

51. Liang, J.; Zeng, G.M.; Shen, S.; Guo, S.L.; Li, X.D.; Tan, Y.; Li, Z.W.; Li, J.B. Bayesian approach to quantify parameter uncertainty and impacts on predictive flow and mass transport in heterogeneous aquifer. *Int. J. Environ. Sci. Technol.* **2015**, *12*, 919–928. [CrossRef]

52. Jie, L.; Xun, Y.; Zeng, G.; Wu, H.; Dai, J. A hydrologic index based method for determining ecologically acceptable water-level range of Dongting Lake. *J. Limnol.* **2014**, *73*, 75–84.

53. Xiao, R.; Guo, D.; Ali, A.; Mi, S.; Liu, T.; Ren, C.; Li, R.; Zhang, Z. Accumulation, ecological-health risks assessment, and source apportionment of heavy metals in paddy soils: A case study in Hanzhong, Shaanxi, China. *Environ. Pollut.* **2019**, *248*, 349–357. [CrossRef]

54. Singh, U.K.; Ramanathan, A.L.; Subramanian, V. Groundwater chemistry and human health risk assessment in the mining region of East Singhbhum, Jharkhand, India. *Chemosphere* **2018**, *204*, 501–513. [CrossRef]